Journal of Applied Mechanics and Technical Physics, Vol. 37, No. 4, 1996

INTERACTION OF A SHOCK WAVE WITH A CLOUD OF PARTICLES WITH DISTURBED BOUNDARIES

S. P. Kiselev and V. P. Kiselev

UDC 662.612.32

The results of a numerical simulation of the interaction between a shock wave (SW) and a cloud of particles with initially disturbed boundaries are presented in this paper. It is shown that instability develops in the course of time which causes growth of disturbances and damage of the cloud.

Let us consider a cloud of solid particles which occupies region Ω_2 (Fig. 1) and on which an SW is incident from the left. The boundaries of the cloud for $t = 0$ are defined by the equation

$$x_{1,2} = x_{1,2}^0 + a_0 \cos(2\pi y/\lambda),$$

where subscript 1 indicates the front boundary, and subscript 2 the rear boundary; the first component determines the coordinate of the undisturbed boundary, and the second corresponds to disturbances with amplitude a_0 and wavelength λ.

The vertical size of the cloud is selected so that two disturbance wavelengths are present along it. Region Ω_1 is occupied by a gas whose behavior is described by Euler equations, and Ω_2 by a mixture of the gas with the particles. The flow of the gas–particles mixture is given by the equations of a continuum-discrete model; the algorithm for their numerical solution is presented in [1]. The wall condition was specified for the gas at the boundaries γ_1 and γ_3, and the condition of a zero gradient of gasdynamic functions at γ_2 and γ_4. Specular reflection was assumed for γ_1 and γ_3, and particle absorption, for γ_2 and γ_4 (Fig. 1).

Ahead of the SW the gas (air) was under normal conditions: $\gamma = 1.4$, $\rho_0 = 1.2 \cdot 10^{-3}$ g/cm^3, $p_0 = 1$ atm (γ is the specific heat ratio, ρ_0 and p_0 are the initial gas density and pressure), and the gas parameters behind the SW were determined from the Hugoniot relation. The SW Mach number was $M_0 = 2.7$ ($M_0 = D/c_0$ and D is the SW velocity). Plexiglas particles were used for calculations (particle diameter $d = 2 \cdot 10^{-3}$ cm, volume concentration $m_2^0 = 3 \cdot 10^{-2}$, and $m_2 = \pi d^3 n/6$, where n is the particle concentration). The initial thickness of the cloud was $h_0 = 1$ cm ($h_0 = x_2^0 - x_1^0$), the amplitude of the disturbance was $a_0 = 0.15$ cm, and the wavelength was $\lambda = 1.45$ cm.

The interaction of the SW with the cloud of particles results in the formation of a reflected SW, a transmitted transient wave, and a rarefaction wave (Fig. 2 shows isobars in atmospheres for $t = 80$ μsec; the dashed curves indicate the boundaries of the cloud). It is seen that the rarefaction wave is located inside the cloud and does not spread with time [1]. The gas flow is subsonic behind the reflected SW. When convex regions of the cloud (disturbance maxima) are in the flow, the stream is compressed, which leads to gas acceleration and growth in the dynamic pressure $\rho v_1^2/2$ in the regions of disturbance minima (ρ and v_1 are the gas density and velocity, respectively). Since the force $f = (\pi d^2/8) C_d \rho v_1^2$ acting on the particle is proportional to the dynamic pressure, the value of f is larger in the region of disturbance minima than in the region of their maxima. This leads to the growth of disturbances.

Another important feature of the growth of disturbances and break of cloud is the presence of secondary flows. It is seen from Fig. 2 that the isobars in the cloud follow the cloud contours. As a result, a nonzero

Institute of Theoretical and Applied Mechanics, Siberian Division, Russian Academy of Sciences, Novosibirsk 630090. Translated from Prikladnaya Mekhanika i Tekhnicheskaya Fizika, Vol. 37, No. 4, pp. 36–39, July–August, 1996. Original article submitted May 10, 1995.

 0021-8944/96/3704-0488 $15.00

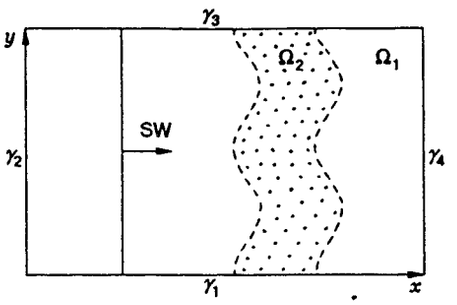

Fig. 1

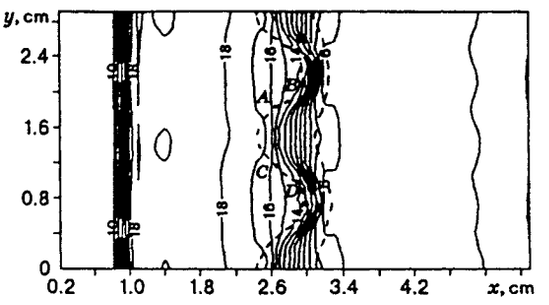

Fig. 2

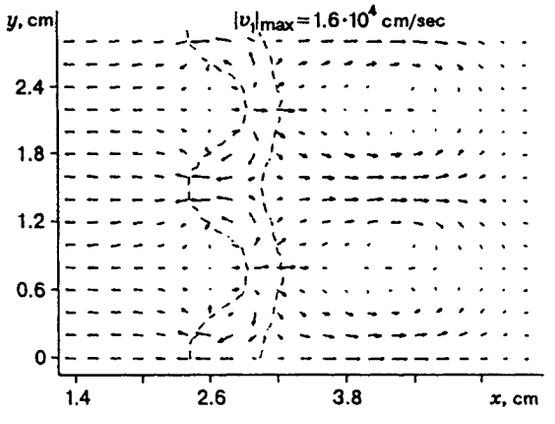

Fig. 3

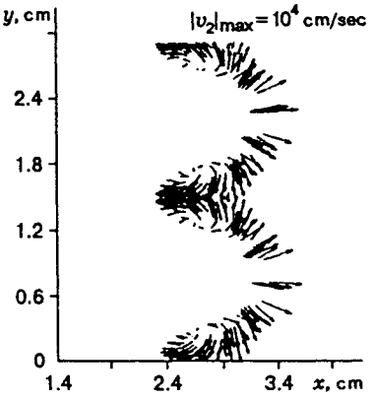

Fig. 4

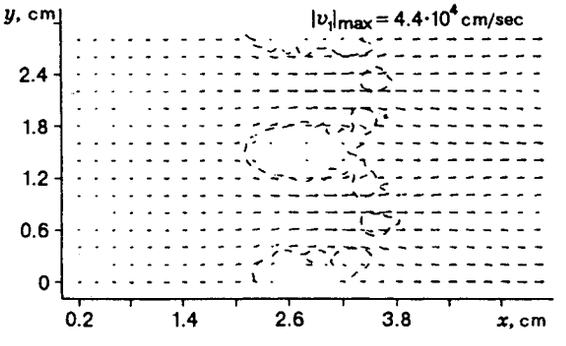

Fig. 5

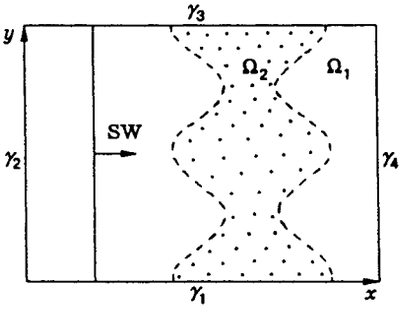

Fig. 6

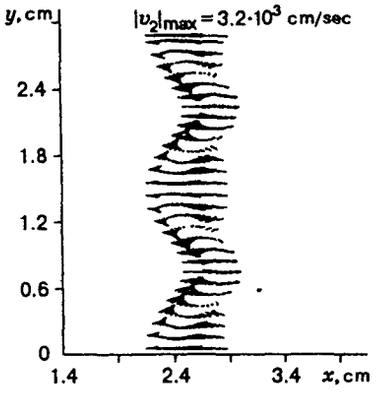

Fig. 7

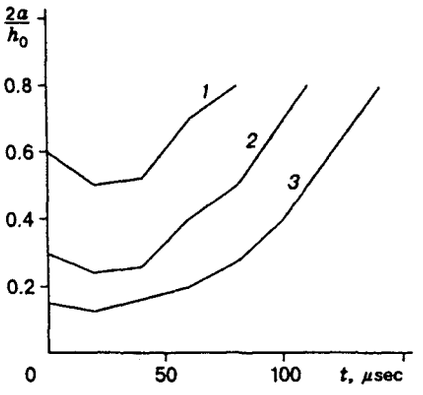

Fig. 8

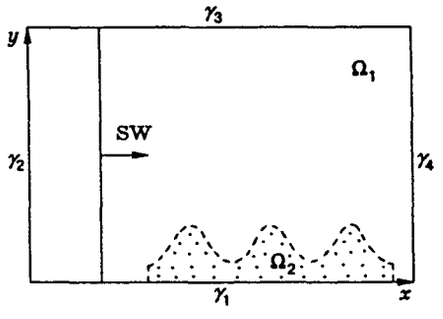

Fig. 9

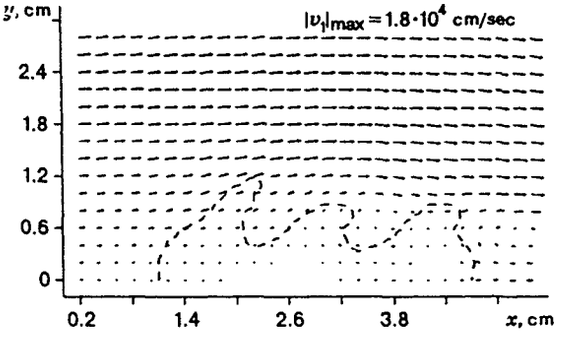

Fig. 10

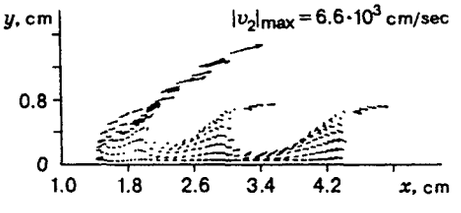

Fig. 11

component ∇p directed inside the cloud appears on the convex boundaries of the cloud (see, for instance, regions AB and CD in Fig. 2). Under the action of ∇p, the gas flows into the cloud and swirls as four vortices.

Figure 3 shows the gas-velocity field for $t = 80$ μsec in the coordinate system fixed with the moving gas: $v'_{1x} = v_{1x} - u$ and $v'_{1y} = v_{1y}$, $u = \int \rho v_{1x} dV / \int \rho dV$, ($v_{1x}$, v_{1y} are the gas-velocity components in the laboratory coordinate system). One can see that two vortices in the cloud and two vortices outside the cloud are present along the wavelength λ. Under the action of friction forces, the particles are entrained in the gas vortex. Thus, the particles are removed from the minimum regions to the maximum regions, and the cloud breaks up into separate bunches.

Figure 4 shows the particle-velocity field v_2 for $t = 100$ μsec, which illustrates the particle motion pattern described above, and the gas-velocity field in the cloud-fixed system after the break-up of the cloud into bunches is presented in Fig. 5 ($t = 140$ μsec). A similar development of disturbances is observed for an initial volume concentration $m_2^0 = 10^{-3}$. However, the disturbances grow less rapidly in this case, and, therefore, the cloud is not destroyed. The particle velocity reaches the gas velocity before the cloud breaks up.

The secondary vortex flows described above can change significantly the cloud configuration. Let the initial cloud boundaries be such as in Fig. 6. At $t = 0$, the cloud has volume concentration $m_2^0 = 10^{-3}$, $a_0 = 0,3$ cm, and the particle and SW parameters are the same as above. After SW passage and vortex formation, the rear cloud boundary is first smoothed (Fig. 7) and then becomes geometrically similar to the front boundary, as is shown in Fig. 1. Similar calculations for $m_2^0 = 3 \cdot 10^{-2}$ show that the rear boundary tends to follow the front boundary. This process is not completed, however, because of a break in the minimum cross-section of the cloud.

The growth rate of disturbances depends on particle diameter d, volume concentration m_2^0, and on the SW strength and weakly depends on cloud thickness h_0. Figure 8 shows the curve of $2a/h_0$ (a is the amplitude of disturbances) in time for three initial disturbance amplitudes $a_0 = a|_{t=0}$ (curves 1–3 correspond to $a_0 = 0.075$, 0.15, and 0.3 cm). The dependence $a(t)$ is approximately exponential with attainment of a constant growth rate of disturbances. Some valley at $t \approx 40$ μsec is due to the difference between the times of SW arrival at the minima and maxima of disturbances. In the region of disturbance maxima, the particles stay in the gas flow for a longer time than in the region of disturbance minima, and, therefore, the amplitude is reduced for $t \leqslant 40$ μsec. Instability is further developed, and the growth of disturbances begins to dominate.

Let us now consider a cloud of particles whose upper boundary is disturbed according to the formula $y = y_0 + a_0 \cos(2\pi x/\lambda - \pi)$. An SW approaches the cloud from the left (Fig. 9); $M_0 = 1.3$, $m_2^0 = 3 \cdot 10^{-2}$, $a_0 = 0.3$ cm, $\lambda = 1.3$ cm, and $y_0 = 0.65$ cm. The remaining parameters are the same as above. The gas-velocity field is shown in Fig. 10 for $t = 250$ μsec, and the particle-velocity field is presented in Fig. 11 for $t = 400$ μsec. It is seen that the gas, meeting an obstruction in the form of the cloud of particles, is decelerated due to the viscous interaction with the particles and turns upward. As a result, the particles are removed from the front part of the cloud into the outer region. A vortex flow forms between adjacent cloud crests and entrains the particles. In the maxima region of the disturbance wave, the particles are entrained in the external flow and pulled downstream.

We should note in conclusion that the above picture of growth disturbances of the cloud boundaries and damage of the cloud is in qualitative agreement with that observed experimentally [2, 3].

REFERENCES

1. V. P. Kiselev, S. P. Kiselev, and V. M. Fomin, " Interaction of a shock wave with a cloud of particles of finite dimensions," *Prikl. Mekh. Tekh. Fiz*, **35**, No. 2, 26–37 (1994).
2. V. M. Boiko, A. V. Fedorov, V. M. Fomin, et al, "Ignition of small particles behind shock waves," in: *Shock Waves, Explosion, and Detonations, Ser. Progress in Astronautics and Aeronautics*, **87**, New York, AIAA Publ. (1983), pp. 71–87.
3. V. M. Boiko and A. N. Papyrin, "Dynamics of gas mixture formation behind a shock wave sliding along the granular medium surface," *Fiz. Goreniya Vzryva*, **23**, No. 2, 122–126 (1987).